River Flow 2010 - Dittrich, Koll, Aberle & Geisenhainer (eds) - © 2010 Bundesanstalt für Wasserbau ISBN 978-3-939230-00-7

2D-H Numerical Simulation of Dam-Break Flow on Mobile Bed with Sudden Enlargement

M. Iervolino
Dept. of Civil Engineering, Seconda Università degli Studi di Napoli; Real Casa dell'Annunziata, via Roma 29, 81031 Aversa (CE), Italy.

A. Leopardi
Dept. of Mechanics, Structures and Environmental Engineering (DiMSAT), Università degli Studi di Cassino; via G. Di Biasio 43, 03043 Cassino (FR), Italy.

S. Soares-Frazão & C. Swartenbroekx
Fonds National de la Recherche Scientifique and Dept. of Civil Engineering, Université catholique de Louvain; place du Levant, 1, B-1348 Louvain-la-Neuve, Belgium.

Y. Zech
Dept. of Civil Engineering, Université catholique de Louvain; place du Levant, 1, B-1348 Louvain-la-Neuve, Belgium.

ABSTRACT: The failure of a major flood control structure may expose the surrounding population to serious risk. Such an event kind may involve rapid transients with strong interactions between flow and topography. Similar morphodynamical processes may then exhibit a behavior not explainable using the hypothesis of immediate adaptation of solid transport to flow condition. So, to correctly simulate the consequences of a dam failure in a complex topography, this interaction should be accounted for in mathematical modeling, which should however rely on physical descriptions that are not yet completely established. Within this framework, accurate experimental data in idealized cases are essential to clarify the process evolution and to validate mathematical and numerical models still in development. In the present paper, recent experiments realized in a channel with a sudden enlargement are used for comparing results of a morphodynamical model with an explicit dynamical description of sediment transport, against a classical Saint Venant – Exner model. Such an enlargement features some interesting particularities, with zones with highly curved flow filaments with high curvature and strong erosion and shadowed zones behind the enlargement.

Keywords: Dam-break wave, Bed-load transport, Sediment inertia, Two-phase flow, Enlargement

1 INTRODUCTION

The failure of a major flood control structure as a dam constitutes a risk for the surrounding population. During such a hazard involving rapid transients, interaction between flow and bed can be significant. For example, the 1996 Lake Ha !Ha ! breakout flood in Québec severely reshaped the downstream valley (Capart et al. 2007). To predict correctly the consequences of a dam failure in a complex topography, the interaction between flow and bed must be carefully modeled. Accurate experimental data in idealized cases are, therefore, essential to understand the phenomenon and to validate numerical models.

Earlier dam-break flow experiments were executed with clear-water on fixed bed in one-dimensional configurations (e.g. Dressler 1954) or with two-dimensional features (e.g. Bell et al. 1992, Bellos et al. 1992, Aureli et al. 2004). Among the first laboratory studies concerning sand and gravel mobile bed, the investigation of Chen & Simons (1979) highlighted the effect of river sinuosity and deposited sediments after the failure of a dam. Capart & Young (1998) used lightweight artificial pearls of uniform size as bed material in a horizontal flume. The authors discovered that the dam-break wave, just after its release, excavates a growing scour hole and forms a hydraulic jump which propagates upstream with time. Leal et al. (2002) compared the propagation of dam-break waves on fixed, pumice and sand bed in a horizontal flume. Spinewine & Zech (2007) realized dam-break experiments on sand and PVC bed featuring a level discontinuity at the location of the gate. Soares-Frazão et al. (2007) executed their test in half a channel presenting banks. Pioneer experiments of a two-dimensional dam-break flow, i.e. a sudden enlargement on a mobile bed, were analyzed by Palumbo et al. (2008) and by Goutière et al. (submitted).

In order to simulate mobile-bed dam-break problems, the simpler numerical models used a shallow-water formulation of mass balance of each phase, i.e. liquid and solid phase, and momentum balance for the whole mixture. The solid phase description often reduced to bed time evolution following erosion and deposition, neglecting both the suspended load and the inertia effects of the moving sediment phase. Assuming hydrostatic pressure, incompressible fluid and small slope, the Saint-Venant-Exner set of equations are obtained (Lyn & Altinakar 2002). These models are closed with formulas for hydraulic slope and for bed-load transport. A failure operator can be included to predict bank morphological evolution (Spinewine et al. 2002, Swartenbroekx et al. submitted).

These classical models based on Saint-Venant-Exner equations usually assumed that the solid transport capacity equals the actual solid transport. However, Armanini & Di Silvio (1988) showed the importance of non-equilibrium equation to calculate the flux through the bottom surface at short time-scale. They assumed a spatial lag between the transport capacity and the actual sediment discharge, defining a characteristic length for which empirical formulations exist or which has to be calibrated.

To take into account the inertia of the sediments, several authors proposed to express the momentum balance of all the sediments, leading either to a two-layer model (e.g. Fraccarollo & Capart 2002, Spinewine and Zech 2005, Chen et al. 2007, Savary & Zech 2007) or to a two-phase model (e.g. Jha & Bombardelli 2007, Greco et al. 2008a & b). Two-phase approach considers the sediment as a phase sharing the same space as water, so that in each point of the flow either liquid or solid may exist. While the classical approach (with Saint-Venant-Exner equations) assumes that the solid discharge is determined by the uniform flow formulas, a two-phase model is based on the physical description of dynamic principles applied to the sediment phase. Sediment transport thus progressively adapts to hydrodynamics. Moreover, the closure in terms of erosion flux could in principle address bank failure without any further operator.

2 MODELLING DAM-BREAK FLOW ON MOBILE BED

2.1 *The Saint-Venant-Exner (SVE) Model*

The Saint-Venant shallow-water equations describe mass and momentum conservation for water. The Exner equation states mass conservation for the sediment in the bed, and describes the evolution of the bed level following erosion or deposition. These equations can be written in vector form as (see Soares-Frazão & Zech 2010 for additional details)

$$\frac{\partial \mathbf{U}}{\partial t} + \frac{\partial \mathbf{F}(\mathbf{U})}{\partial x} + \frac{\partial \mathbf{G}(\mathbf{U})}{\partial y} = \mathbf{S} \tag{1}$$

with vectors **U**, **F**, **G** and **S** defined as follows

$$\mathbf{U} = \begin{pmatrix} h \\ uh \\ vh \\ z_b \end{pmatrix} = \begin{pmatrix} h \\ q_x \\ q_y \\ z_b \end{pmatrix}, \quad \mathbf{S} = \begin{pmatrix} 0 \\ gh\left(S_{0,x} - S_{f,x}\right) \\ gh\left(S_{0,y} - S_{f,y}\right) \\ 0 \end{pmatrix} \tag{2a, b}$$

$$\mathbf{F} = \begin{pmatrix} q_x \\ q_x^2/h + gh^2/2 \\ q_x q_y / h \\ q_{s,x}/(1-p) \end{pmatrix}, \quad \mathbf{G} = \begin{pmatrix} q_y \\ q_x q_y / h \\ q_y^2/h + gh^2/2 \\ q_{s,y}/(1-p) \end{pmatrix} \tag{2c, d}$$

where t is time, x and y the space coordinates, g the gravitational acceleration, h the water depth, u and v the depth-averaged velocity components in the x and y directions, respectively, q_x and q_y the unit discharge components, z_b the erodible bed elevation, $q_{s,x}$ and $q_{s,y}$ the components of the sediment transport rate per unit width and p the bed porosity. In the source term vector **S**, $S_{0,x}=\partial z_b/\partial x$ and $S_{0,y}=\partial z_b/\partial y$ are the bed slope in the x and y directions, respectively, and $S_{f,x}$ and $S_{f,y}$ the friction slope components. The friction slope is calculated by the Manning formula. The sediment transport rate q_s is calculated using a closure relation. Here the Meyer-Peter and Müller (MPM) formula, initially developed for one-dimensional flows, is used, because it appeared to be reasonably well suited for the experimental test of the enlargement:

$$q_s(q,h) = 8\sqrt{g\,\Delta\, d_{50}^3}\left(\max\left(0, \tau_* - \tau_{*c}\right)\right)^{3/2} \tag{3}$$

where ρ and ρ_s are the water and sediment density, respectively, $\Delta = (\rho_s-\rho)/\rho$, d_{50} is a representative grain diameter, τ_* denotes the non-dimensional bed shear stress and τ_{*c} the non-dimensional critical bed shear stress. It is considered that sediment start to move when τ_* exceeds the threshold value τ_{*c} (about 0.047). The non-dimensional bed shear stress is calculated as

$$\tau_* = \frac{n^2 q^2}{\Delta d_{50} h^{7/3}} \tag{4}$$

where $q = \sqrt{q_x^2 + q_y^2}$ and n is the Manning friction coefficient.

2.2 *The Greco et al. model*

The morphodynamical model proposed by Greco et al. (2008) is here used. It is a two-phase model, whose equations express, in a depth averaged framework, mass and momentum conservation with reference to water and sediments separately.

Water and sediment mass conservation equations are:

$$\frac{\partial h}{\partial t}+\frac{\partial}{\partial x}(Q_x+Qs_x)+\frac{\partial}{\partial y}(Q_y+Qs_y)+\frac{\partial z_b}{\partial t}=0 \qquad (5)$$

$$\frac{\partial \delta}{\partial t}+\frac{\partial Qs_x}{\partial x}+\frac{\partial Qs_y}{\partial y}+(1-p)\frac{\partial z_b}{\partial t}=0 \qquad (6)$$

in which the same notations as in Section 2.1 are used, except for Q_x and Q_y (Qs_x and Qs_y) the two components of liquid (solid) discharge along x and y, respectively, z_b the bottom elevation above a datum, and δ the ratio of sediment volume to base area.

Water and sediment momentum equations are:

$$\frac{\partial Q_x}{\partial t}+\frac{\partial}{\partial x}\left(\frac{Q_x^2}{h-\delta}+g\frac{h^2}{2}\right)+\frac{\partial}{\partial y}\left(\frac{Q_xQ_y}{h-\delta}\right)+gh\left(\frac{\partial z_b}{\partial x}+Sf_x\right)=0 \qquad (7)$$

$$\frac{\partial Q_y}{\partial t}+\frac{\partial}{\partial x}\left(\frac{Q_xQ_y}{h-\delta}\right)+\frac{\partial}{\partial y}\left(\frac{Q_y^2}{h-\delta}+g\frac{h^2}{2}\right)+gh\left(\frac{\partial z_b}{\partial y}+Sf_y\right)=0 \qquad (8)$$

$$\frac{\partial Qs_x}{\partial t}+\frac{\partial}{\partial x}\left(\frac{Qs_x^2}{\delta}+\frac{g\Delta}{C(\Delta+1)}\frac{\delta^2}{2}\right)+\frac{\partial}{\partial y}\left(\frac{Qs_xQs_y}{\delta}\right)+ \qquad (9)$$
$$+g\delta\frac{\Delta}{\Delta+1}\frac{\partial z_b}{\partial x}+Ss_x=0$$

$$\frac{\partial Qs_y}{\partial t}+\frac{\partial}{\partial x}\left(\frac{Qs_xQs_y}{\delta}\right)+\frac{\partial}{\partial y}\left(\frac{Qs_y^2}{\delta}+\frac{g\Delta}{C(\Delta+1)}\frac{\delta^2}{2}\right)+ \qquad (10)$$
$$+g\delta\frac{\Delta}{\Delta+1}\frac{\partial z_b}{\partial y}+Ss_y=0$$

where S_{fx} and S_{fy} (S_{sx} and S_{sy}) denote the water (sediment) momentum source/sink terms in x and y directions, respectively, and C is the solid concentration (assumed as a constant).

The water source term is the sum of the bottom friction (evaluated using a uniform flow formula) and the drag exchanged between the two phases. The corresponding solid source terms account for drag exchange, Mohr-Coulomb friction and collisional shear stresses, which are evaluated, after Bagnold, as a coefficient α multiplied by the square of the particle velocity.

The seventh and last equation relates the bottom evolution to the mass exchange with the flow, e_b and reads:

$$\frac{\partial z_b}{\partial t}=-e_b \qquad (11)$$

Clearly system (5)-(11) can be written in the same vector form of (1).

A closure relation for the entrainment/deposition term e_b is then required. In order to better compare with previously described SVE model, e_b is expressed through a linear lag relation, evaluating the transport capacity Qs_{MP} of the flow by Meyer Peter and Muller formula.

$$e_b=\frac{Qs_{MP}-Qs}{L*} \qquad (12)$$

Model parameters are then the drag coefficient (Cd), that accounts for the momentum transfer between water and solid phases, the Bagnold α coefficient, the non-dimensional Chezy coefficient (Ch) the friction angle (φ) and the entrainment adaptation length (L_*). More details are given in the original paper by the Authors.

Equations (5) – (11) are a system of conservation laws. As demonstrated by Greco et al. (2008), the system is strictly hyperbolic, which is an essential requirement for well-posedness of the problem in the case of a multi-phase model (Stewart and Wendroff, 1984).

In the following, both PDE systems, eq. (1) and eqs. (5) - (11) have been numerically solved by means of a finite-volume discretisation. The achievement of reasonably grid independent solutions has been checked before the comparison with experimental results.

3 DAM-BREAK FLOW ON MOBILE BED WITH A SUDDEN ENLARGEMENT

3.1 *Experimental results*

Experiments of dam-break flow over movable bed were carried out at the Hydraulic Laboratory of the Université catholique de Louvain (Belgium). These experiments are reported by Palumbo et al. (2008) and Goutière et al. (submitted).

The tests were performed in a 6 m long flume, presenting a non-symmetrical sudden widening, from 0.25 m to 0.5 m width, located 1 m downstream of the gate (Figure 1). The breaking of the dam is simulated by the rapid downward movement of a thin gate at the middle of the flume. The opening of the gate is achieved in a time of about 0.1 s. The sediment used is a uniform coarse sand with a median diameter d_{50} of 1.72 mm and relative density of $\Delta+1 = 2.63$, deposited with a bulk concentration of 39.22% (Becker and Kaiser,

2008). The initial conditions consist of a 0.1 m high horizontal layer of fully saturated and compacted sand over the whole flume, and an initial layer of 0.25 m clear water upstream of the gate (Figure 1).

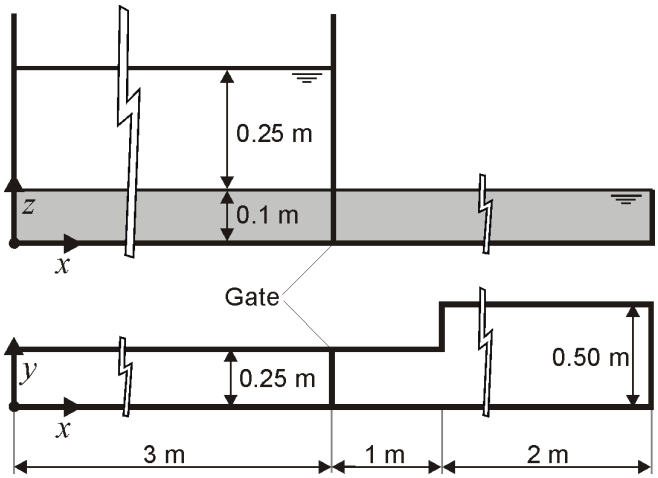

Figure 1. Experimental set-up and initial conditions.

The measurements of the flow depth and the final bed topography were performed with nonintrusive techniques: ultrasonic gauges and digital imagery. The evolution in time of the water level is provided by 8 ultrasonic gauges placed downstream of the gate as sketched in Figure 2. The morphological changes generated by the flow were measured at the end of the experiment. A laser sheet imaging technique, described in Soares-Frazão et al. (2007), has been used to measure the shape of successive cross-sections in the enlarged part of the channel (Figure 3).

The main observations of the experiments are here recalled. After the opening of the gate, a water and sediment wave propagates in the downstream direction and progressively spreads over the wider region of the flume. This rapid flow generates intense erosion and a scour hole develops at the inner corner of the widening. Progressively, the water spreads in the wider reach of the flume and reflects against the left sidewall. This reflection generates an oblique hydraulic jump and a recirculation area is created in the outside corner of the widening. The final topography displays a deposition crest in the left part of the wider region while erosion is visible between the left sidewall and the deposition crest.

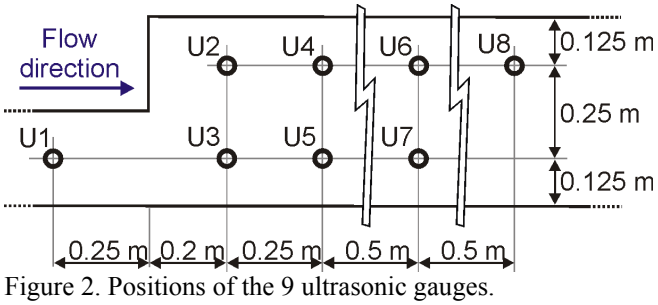

Figure 2. Positions of the 9 ultrasonic gauges.

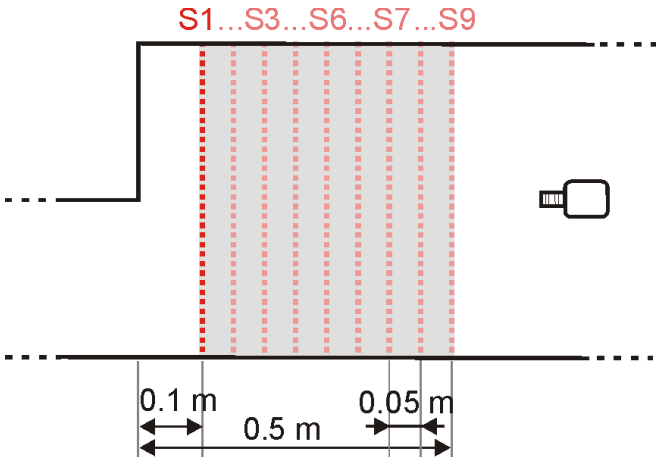

Figure 3. Positions of the 9 cross-sections analyzed by the laser-sheet imaging technique.

3.2 *Numerical results*

The experiment described in the previous section was simulated using the morphodynamical models described above, namely the SVE and the two-phase dynamical one. The values of the parameter in the source terms of the two-phase model have been chosen as the ones which appeared to provide the best agreement with the experimental data.

It is worth of note that, due to the lack of knowledge on the evaluation of the adaptation length in similar flow conditions, a constant value $L^* = 10^{-1}$ m has been adopted, based on the relevant lengthscales of flow.

For both models, simulated time histories and final bed configuration were computed in the locations corresponding to the experimental devices.

The achieved results in terms of time histories of water surface elevation and final bottom configurations are depicted in Figures 4 and 5, respectively. Experimental results are plotted as solid lines, while void (filled) symbols represent the results of the equilibrium (dynamical) model.

3.3 *Comparison and discussion*

The examination of the results represented in Figure 4 shows that the overall behavior of the flow is well captured by both models, but a deeper analysis reveals the inherent complexity of the investigated flow field. Several bores appear on the experimental water surface, especially at the gauges located close to the expansion zone, up to the position of U6 gauge. None of the models is able to accurately capture the sudden increase or decrease of the water surface level, even if a slightly better agreement can be observed for the dynamical model for gauge U3.

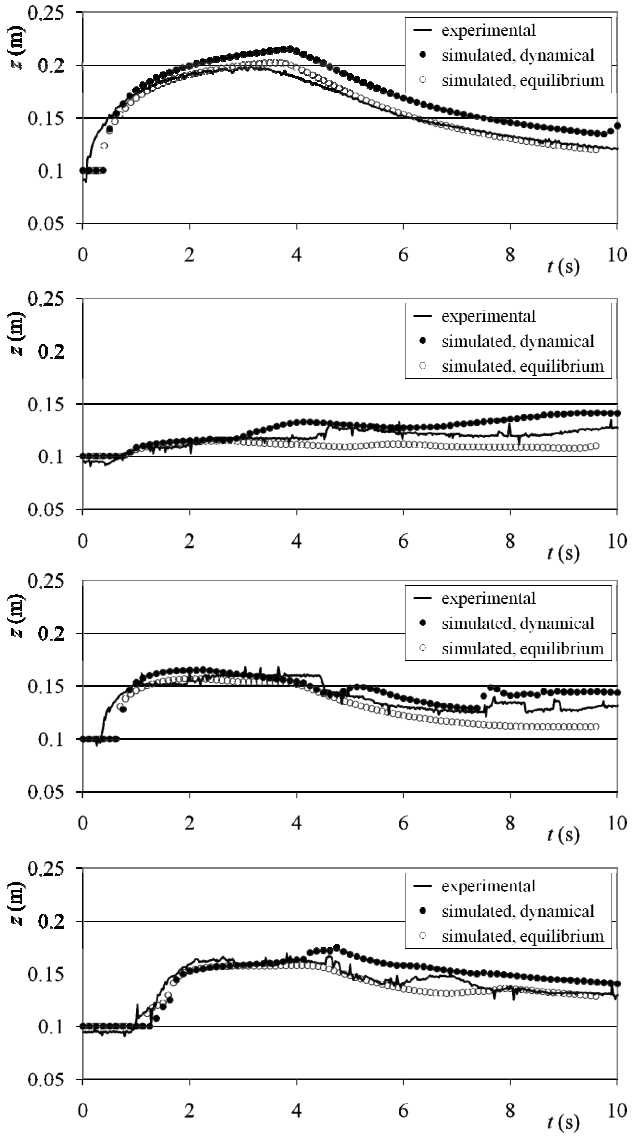

Figure 4. Experimental and simulated time histories of water surface elevation. From top to bottom: gauge U1, U2, U3 and U6.

A more detailed comparison should require spatially distributed observations of the two-dimensional configuration of bores, which are not available from the experiments.

The final bottom configuration of the bottom is characterized by two main geomorphic features: a major deposit in the downstream-looking left half of the wide channel (see Figure 1 for the axis convention), and an intense scour close to the middle of the wide channel, both clearly noticeable in the interval bounded by S1 and S7 sections.

Moving downstream, the height of the deposit grows up to about $2 \cdot 10^{-2}$ m, and its crest moves approximately from $y = 0.3$ m (S1) to $y = 0.4$ m (S7). On the other hand, the flow curvature near the sudden enlargement causes an excavation of about $3 \cdot 10^{-2}$ m in S1, with a pronounced scour hole close to the middle of the wide channel. Moving downstream, the shape of the scour tends to flatten, so that in S7 the minimum can be hardly noticed.

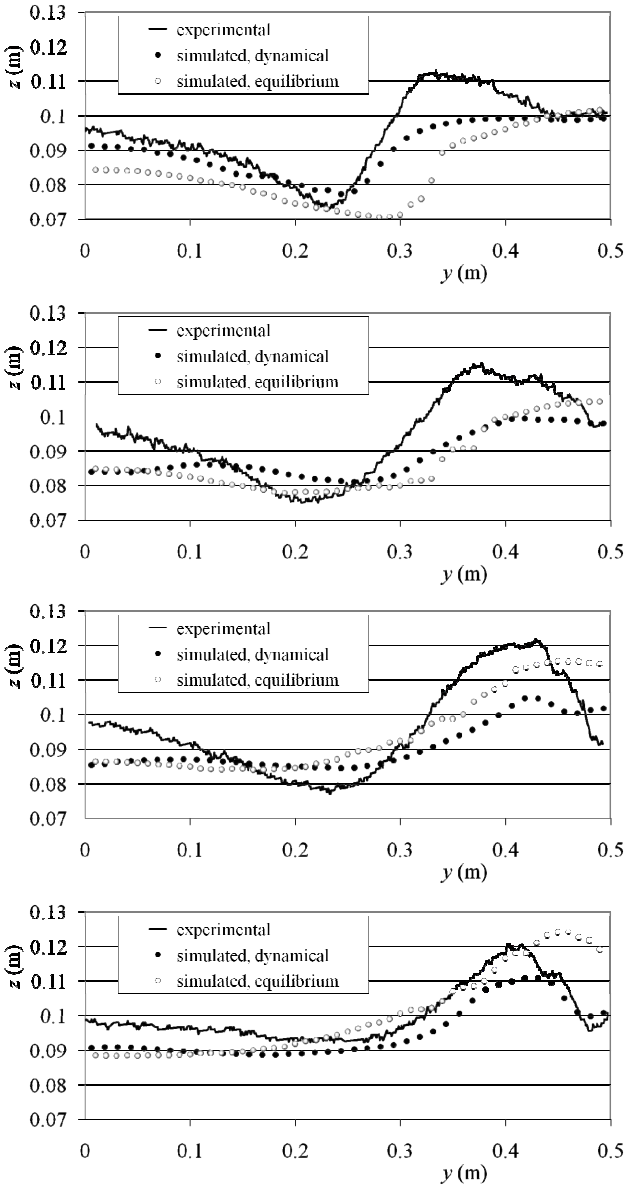

Figure 5. Experimental and simulated cross-sections of final bottom elevation. From top to bottom: section S1, S3, S5 and S7.

When looking at the simulated results, the qualitative shape of the bed is somewhat respected, but again some differences still can be observed. A common feature for both models is that the deposit takes place on a distance longer than the experimentally observed. Such a spatial lag is witnessed by the fact that in section S1 no appreciable deposit exists.

As far as the equilibrium model is concerned, the deposition seems to be triggered by the sudden arrest of the sediment, caused by to the impact with the right sidewall. By contrast, the deposit predicted by the dynamical model, similarly to the observed one, does not reach the right sidewall in any of the cross-sections. A possible explanation of this behavior is that deposition may be caused by particle friction rather than by the decrease of the shear stress of the carrying flow, which ac-

companies the formation of an oblique hydraulic jump as the dam-break wave hits the sidewall.

Concerning the shape of the scoured zone, both models predict the return to a quasi-flat bed in a reach shorter than the observed one. The dynamical adaptation of the solid transport seems to allow to predict more accurately the position of the maximum scour in the section S1, but the differences in the final bottom topography become almost negligible after the section S5.

From the above analysis, the present test-case still appears to be a really challenging test for morphodynamical model, especially as far as the quantitative agreement is concerned. Despite the inclusion of physically-based modeling of non-equilibrium transport seems to lead to some improvement, further research, both experimental and theoretical, is needed to understand the physics of such kind of complex geomorphic flows.

4 CONCLUSION

In the paper recent experiments realized in a channel with a sudden enlargement have been used to compare results of a classical Saint Venant – Exner model with a two-phase morphodynamical model with an explicit dynamical description of sediment transport. This morphodynamical two-phase model separately expresses, in a depth averaged framework, mass and momentum conservation for water and sediments.

Experiments of dam-break flow over movable bed were carried out at the Hydraulic Laboratory of the Université catholique de Louvain (Belgium). The considered experiment exhibits some interesting particularities, with zones with highly curved flow filaments with high curvature and strong erosion and shadowed zones behind the enlargement.

When looking at the simulated results, the qualitative behavior of the flow is reasonably reproduced by both models, but quantitative differences respect to the observed features can be observed, both in the transient and in the final stage of the process. For instance, both models predict that sediment deposition takes place on a distance longer than the experimentally observed. Concerning the scoured zone, both models underestimate the length of the reach needed to reach a quasi-flat bed in the smallest positive-y half of the wide channel. However, the dynamical adaptation of the solid transport seems to allow to predict more accurately the position of the maximum scour, but the differences in the final bottom topography become almost negligible as soon as we move away from the enlargement zone. In other words the dynamical model seems permit a better reproduction of the whole process but the final bottom configuration can be previsied in a reasonable manner also using the classical model.

We may therefore conclude that the present test-case still appears to be a really challenging test for morphodynamical models. Further research, both experimental and theoretical, is needed to understand the physics of such a complex geomorphic flows.

REFERENCES

Armanini, A., Di Silvio, G. 1988. A one-dimensional model for the transport of a sediment mixture in non-equilibrium conditions. Journal of Hydraulic Research, IAHR, Vol. 26(3), 275-292.

Aureli, F., Maranzoni, A. Mignosa, P. 2004. Experimental modelling of rapidly varying flows on wet bed and in presence of submersible obstacles. Proc. of River Flow 2004 Greco, M. et al. (eds), Napoli, Italy.

Becker, A., Kaiser, D. 2008. Ecoulement consécutif à une rupture de barrage dans un canal présentant un élargissement brusque : mesures de la surface libre et de la topographie finale (in French). MSc thesis, Université catholique de Louvain, Louvain-la-Neuve, Belgium.

Bell, S.W., Elliot, R.C., Chaudhry, M.H. 1992. Experimental investigation of two-dimensional dam-break induced flows. Journal of Hydraulic Research, IAHR, Vol. 30(2), 225-252.

Bellos, C. V., Soulis, J.V., Sakkas, J.G. 1992. Experimental investigation of two-dimensional dam-break induced flows. Journal of Hydraulic Research, IAHR, Vol. 30(1), 47-63.

Capart, H., Spinewine, B., Young, D.L., Zech, Y., Brooks G.R., Leclerc M., Secretan Y. 2007. The 1996 Lake Ha! Ha! breakout flood, Québec: test data for geomorphic flood routing methods. Journal of Hydraulic Research, IAHR, Vol. 45 Extra Issue, 97-109.

Capart, H., Young, D.L. 1998. Formation of a jump by the dam-break wave over a granular bed. Journal of Fluid Mechanics, Vol. 372, 165-187.

Chen, S.C., Peng, S.H., Capart, H. 2007. Two-layer shallow water computation of mud flow intrusions into quiescent water. Journal of Hydraulic Research, IAHR, Vol. 45(1), 13-25.

Chen, Y.H., Simons, D.B. 1979. An experimental study of hydraulic and geomorphic changes in an alluvial channel induced by failure of a dam. Water Resources Research, Vol. 15(5), 1183-1188.

Dressler, R.F. 1954. Comparison of theories and experiments for the hydraulic dam-break wave. Proc. of International Association of Hydrological Sciences, 38(3), 319-328.

Fraccarollo, L., Capart, H. 2002. Riemann wave description of erosional dam-break flows. Journal of Fluid Mechanics, Vol. 461, 183 – 228.

Goutière L., Soares-Frazão S., Zech Y. Dam-break flow on mobile bed in a channel with a sudden enlargement: experimental data. Submitted to the Journal of Hydraulic Research.

Greco, M., Iervolino, M., Leopardi, A. 2008a. Two-phase depth-integrated model for unsteady river flow. Proc. of the Int. Conf. ICHE-2008: 8th International Conference

on Hydro-Science and Engineering. Nagoya (Japan), 2008

Greco, M., Iervolino, M., Vacca, A., Leopardi, A. 2008b. A two-phase model for sediment transport and bed evolution in unsteady river flow. Proc. of River Flow 2008, Altinakar, M. et al. (eds.), Çeşme, Turkey.

Jha, S.K., Bombardelli, F.A. 2007. Two-phase theoretical and numerical models for sediment-laden, open-channel flow. Proc. of River, Coastal and Estuarine Morphodynamics 2007, Enschede, The Netherlands.

Leal, J.G.A.B., Ferreira, R.M.L., Cardoso, A.H. 2002. Dam-break waves on movable bed. Proc. of River Flow 2002, Bousmar, D. & Zech, Y. (eds.), Louvain-la-Neuve, Belgium.

Lyn, D.A., Altinakar, M. 2002. St. Venant-Exner equations for near-critical and transcritical flows. Journal of hydraulic engineering, ASCE, Vol. 128(6), 579-587.

Palumbo, A., Soares-Frazão, S., Goutière, L., Pianese, D., Zech, Y. 2008. Dam-break flow on mobile bed in a channel with a sudden enlargement, Proc. River Flow 2008 International Conference on Fluvial hydraulics, Altinakar, M. et al. (eds.), Çeşme, 3-5 September 2008, 1, 645-654.

Savary, C. & Zech, Y. 2007 Boundary conditions in a two-layer geomorphological model: application to a hydraulic jump over a mobile bed. Journal of Hydraulic Research, IAHR, Vol. 45(3), 316-332.

Soares-Frazão, S., le Grelle, N., Spinewine, B., Zech, Y. 2007 Dam-break induced morphological changes in a channel with uniform sediments: measurements by a laser-sheet imaging technique, Journal of Hydraulic Research Vol. 45 Extra Issue, 87-95.

Soares-Frazão, S., Zech, Y. 2010. HLLC scheme with novel wave-speed estimators appropriate for two-dimensional shallow-water flow on erodible bed. International Journal for Numerical Methods in Fluids. DOI: 10.1002/fld.2300

Spinewine, B., Capart, H., le Grelle, N., Soares Frazão, S., Zech, Y. 2002. Experiments and computations of bank-line retreat due to geomorphic dam-break floods. Proc. of River flow, Bousmar, D. & Zech, Y. (eds.), Louvain-la-Neuve, September 2002, Vol. 1, 651-661.

Spinewine, B., Zech, Y. 2005. Dam-break on a movable bed in presence of an initial bed discontinuity: laboratory experiments and simulations with a multi-layer shallow water model. Proc. 31st IAHR Congress, Seoul, Korea, 11-16 September 2005, CD-ROM, 3422-3433.

Spinewine, B., Zech, Y. 2007. Small-scale laboratory dam-break waves on movable beds. Journal of Hydraulic Research, IAHR, Vol. 45 Extra Issue, 73-86.

Stewart, H.B., Wendroff, B., 1984. Two-phase flow: models and methods. Journal of Computational Physics, Vol. 56, 363–409.

Swartenbroekx, C., Staquet, R., Soares-Frazão, S, Zech, Y. Two-dimensional operator for bank failures induced by water level rise in dam-break flows. Submitted to the Journal of Hydraulic Research.